NANO LETTERS

2009
Vol. 9, No. 6
2508-2510

Mitochondrial Cristae Revealed with Focused Light

Roman Schmidt,† Christian A. Wurm,† Annedore Punge, Alexander Egner,* Stefan Jakobs,* and Stefan W. Hell*

Max Planck Institute for Biophysical Chemistry, Department of NanoBiophotonics, 37077 Göttingen, Germany

Received May 1, 2009

ABSTRACT

Because of the diffraction resolution barrier, optical microscopes have so far failed in visualizing the mitochondrial cristae, that is, the folds of the inner membrane of this 200 to 400 nm diameter sized tubular organelle. Realizing a ~30 nm isotropic subdiffraction resolution in isoSTED fluorescence nanoscopy, we have visualized these essential structures in the mitochondria of intact cells. We find a pronounced heterogeneity in the cristae arrangements even within individual mitochondrial tubules.

Mitochondria are the powerhouses of all eukaryotic cells. In most cell types, they exist as a dynamic reticulum of long, thin, and branched tubules that spread throughout the cytoplasm of the cell (Figure 1a). Light microscopy has been central to the study of the overall shape and the dynamical behavior of these mitochondrial networks.[1,2] However, all we know about the inner architecture of mitochondria is from electron microscopy, which in the 1950s and 1960s revealed that these organelles assume a tubular shape with an outer and an inner membrane.[3] Typically, mitochondria have a diameter of 200−400 nm, which corresponds to about a third of the light wavelength. Within this narrow space, the highly convoluted inner membrane folds into cristae, which host the oxidative phosphorylation system that is pivotal to the generation of energy in the cell.[4] Optical microscopy has failed in visualizing cristae because discerning details smaller than half the wavelength of light ($\lambda = 400-800$ nm) has been precluded by diffraction.

In the recent past, physical concepts emerged for overcoming the diffraction resolution barrier in lens-based fluorescence microscopy. Having provided three-dimensional (3D) resolution on the nanoscale, these fluorescence nanoscopy methods, namely, stimulated emission depletion (STED),[5,6] photoactivation localization,[7] and stochastic optical reconstruction[8] microscopy have all been successfully applied to imaging mitochondria. Yet the visualization of the cristae, the arguably most challenging structural element

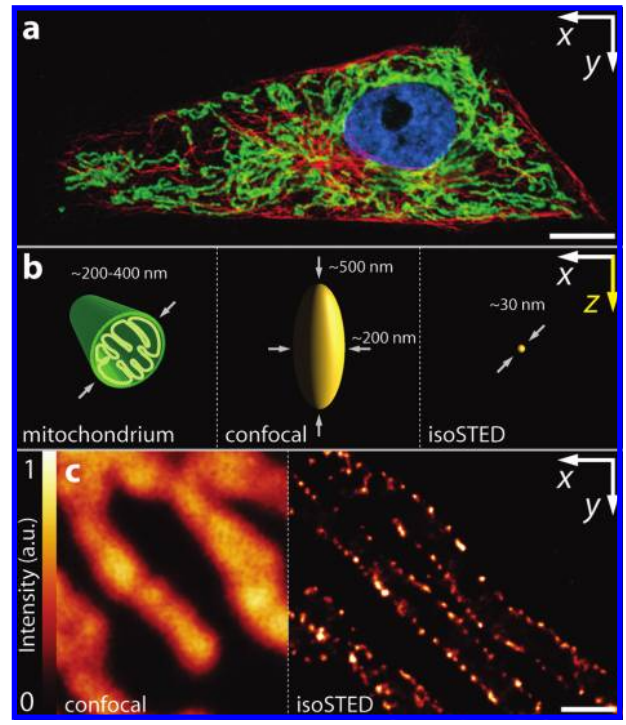

Figure 1. (a) Overview on the mitochondrial network of a PtK2 (kangaroo rat) cell. The mitochondria were labeled with antibodies against the TOM-complex (green) and the microtubule cytoskeleton with antibodies against β-tubulin (red). The nucleus was labeled with DAPI (blue). (b) Sketch comparing the dimensions of a mitochondrial tubule (left) with the confocal (middle) and the isoSTED focal volume (right), drawn to scale. (c) Mitochondria labeled for the outer membrane with antibodies specific for the TOM complex imaged with a confocal microsope (left) or the isoSTED nanoscope (right). The isoSTED raw data were mathematically deconvolved using a maximum likelihood expectation maximization algorithm. Scale bars: 10 μm (a) and 500 nm (c).

* To whom correspondence should be addressed. (S.W.H.) Phone: +49-551-201-2500. E-mail: shell@gwdg.de. (A.E.) Phone: +49-551-201-2555. E-mail: aegner@gwdg.de. (S.J.) Phone: +49-551-201-2531. E-mail sjakobs@gwdg.de.

† These authors contributed equally to this paper.

10.1021/nl901398t CCC: $40.75
Published on Web 05/21/2009

within an organelle for far-field microscopy, has remained elusive.

To visualize the cristae in mitochondria of physically intact cells, we utilized a beam-scanning isoSTED nanoscope[9] featuring a nearly spherical (*iso*tropic) focal spot of fluorescence of ~30 nm diameter, corresponding to ~1/26 of the responsible wavelength of 775 nm. The effective focus was produced by overlapping the excitation spot of two opposing high NA (1.46) oil immersion lenses with a hollow sphere of light for switching off the fluorescence by STED. The resulting focal volume was by about 3 orders of magnitude smaller than that of confocal microscopy and 2−3 times smaller than the volume reported previously (see Supporting Information for more details).[9] Comparison of the dimensions of a mitochondrial tubule with that of the focal volume of a confocal microscope and the isoSTED nanoscope directly indicates that the isoSTED focal volume is sufficiently sharp to reveal details of the mitochondrial interior, whereas the large confocal volume would result in a blurred image (Figure 1b).

The noninvasive all-optical approach of an isoSTED nanoscope, which in essence can be operated like a beam-scanning confocal microscope, allowed us to arbitrarily address any plane inside the cell. To estimate the advantage of the ~30 nm isotropic resolution, we first imaged mitochondria labeled for the translocase of the outer membrane of mitochondria (TOM) complex. Whereas the confocal image fails to provide any details, the isoSTED image reveals individual TOM complexes on the mitochondrial outer membrane (Figure 1c).

To label its run, the mitochondrial inner membrane was marked by immunocytochemistry, attaching fluorophore antibodies labeled with the fluorophore KK114[10] to one of the major protein complexes of the oxidative phosphorylation system within the inner membrane, the F_1F_oATPase. Scanning the tiny isoSTED spot of fluorescence generation through the equatorial plane of a mitochondrion in a cell, embedded in a medium of 97% (v/v) TDE in PBS,[11] clearly delineated the flow of the inner membrane (Figure 2a−c), disclosing cristae as pronounced substructures inside these organelles. Note that because of their strong three-dimensional folding in space the ~30 nm 3D resolution was essential to discern these features.

In general, we found heterogeneous cristae arrangements even within a single mitochondrial tubule (Figure 2a−c). Regions of stacked cristae lamellae alternated with relatively large regions of up to ~10^5 nm^2, which were devoid of cristae. The optical sectioning capability of the nanoscope was especially evident when the mitochondrial tubule crossed the optical plane (Figure 2c). In this case, only the cristae in the focal plane are visible, whereas the fluorescence signals from the remaining mitochondrion are suppressed. In most cases the cristae were perpendicular to the direction of the mitochondrial tubule, but cristae running along the longitudinal axis of the tubule were also observed, underscoring that the arrangement of cristae is highly variable within the

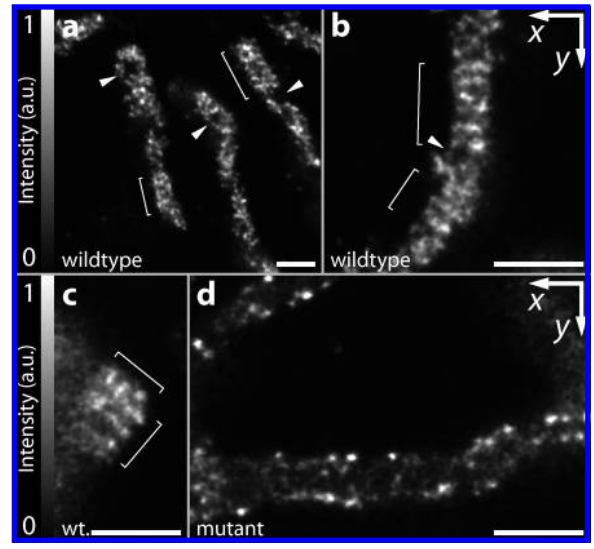

Figure 2. IsoSTED nanoscopy images recorded of mitochondria in the interior of an intact cell revealing the arrangements of cristae. The mitochondrial inner membrane was labeled with antibodies directed against the F_1F_oATPase. (a−c) Wild type PtK2 cells. (a) Overview and (b) close-up of mitochondria recorded at their equatorial planes. (c) Image of a mitochondrion crossing the focal plane. The brackets indicate regions in which the cristae are perpendicularly oriented to the longitudinal axis of the organelle, whereas the arrowheads point to inner-mitochondrial regions devoid of cristae. (d) Mitochondria of a cell depleted for the protein mitofilin, which controls cristae morphology; the distribution of the F_1F_oATPase is altered as a result. The isoSTED raw data were mathematically deconvolved using a maximum likelihood expectation maximization algorithm. Scale bars: 500 nm. The thickness of the all-optical section is about 30 nm.

mitochondria of a single cell. In some tubules, the stacked cristae arrangements extended over several hundred nanometers.

Next, we imaged the distribution of the F_1F_oATPase in mitochondria of cells in which the expression of the mitochondrial protein mitofilin was down regulated by specific small hairpin RNAs (shRNAs). Mitofilin has previously been shown to control cristae morphology.[12] We find that in mitofilin-depleted cells the distribution of the F_1F_oATPase is strongly altered. After mitofilin shRNA transfection, this protein complex is frequently found in large clusters at the rim of the mitochondria and regular cristae are only rarely observed (Figure 2d), fully corroborating the view that depletion of mitofilin results in a disorganized inner membrane.

Finally we mention that numerous severe human diseases are caused by defects in the assembly of the oxidative phosphorylation system in the cristae.[13] The ability to visualize these central structural elements of mitochondria with a beam-scanning light microscope using conventional lenses now paves the way for quantifying their 3D dynamics and that of mitochondrial protein supercomplexes in living cells.

Acknowledgment. We are grateful to Dr. Kirill Kolmakov and Dr. Vladimir Belov for providing us with the new fluorescent dye KK114. We wish to thank Tanja

Gilat and Sylvia Löbermann for excellent technical assistance and Jiping Zha (University of Texas, Dallas) for providing us with the plasmid pAVU6mitofilin. We also acknowledge Jaydev Jethwa and Brian Rankin for critical reading. This work was supported by grants of the Deutsche Forschungsgemeinschaft (JA 1129/3) to S.J. and (SFB 755) to A.E. and S.W.H.

Supporting Information Available: Additional information on the used materials and methods. This material is available free of charge via the Internet at http://pubs.acs.org.

References

(1) Bereiter-Hahn, J.; Voth, M. *Microsc. Res. Tech.* **1994**, *27* (3), 198–219.
(2) Jakobs, S. *Biochim. Biophys. Acta* **2006**, *1763* (5−6), 561–575.
(3) Frey, T. G.; Mannella, C. A. *Trends Biochem. Sci.* **2000**, *25* (7), 319–324.
(4) Saraste, M. *Science* **1999**, *283* (5407), 1488–93.
(5) Hell, S. W.; Wichmann, J. *Opt. Lett.* **1994**, *19* (11), 780–782.
(6) Klar, T. A.; Jakobs, S.; Dyba, M.; Egner, A.; Hell, S. W. *Proc. Nat. Acad. Sci. U.S.A* **2000**, *97*, 8206–8210.
(7) Betzig, E.; Patterson, G. H.; Sougrat, R.; Lindwasser, O. W.; Olenych, S.; Bonifacino, J. S.; Davidson, M. W.; Lippincott-Schwartz, J.; Hess, H. F. *Science* **2006**, *313* (5793), 1642–1645.
(8) Huang, B.; Wang, W.; Bates, M.; Zhuang, X. *Science* **2008**, *319*, 810–813.
(9) Schmidt, R.; Wurm, C. A.; Jakobs, S.; Engelhardt, J.; Egner, A.; Hell, S. W. *Nat. Methods* **2008**, *5* (6), 539–544.
(10) Hell, S. W.; Belov, V. Kolmakov, K.; Westphal, V.; Lauterbach, M. A.; Jakobs, S.; Wurm, C. A.; Eggeling, C.; Ringemann, C. Novel Hydrophilic and Lipophilic Rhodamines for Labelling and Imaging. Eur. Pat. Appl., April 28, **2009**.
(11) Staudt, T.; Lang, M.; Medda, R.; Engelhardt, J.; Hell, S. W. *Microsc. Res. Tech.* **2007**, *70* (1), 1–9.
(12) John, G. B.; Shang, Y.; Li, L.; Renken, C.; Mannella, C. A.; Selker, J. M.; Rangell, L.; Bennett, M. J.; Zha, J. *Mol. Biol. Cell* **2005**, *16* (3), 1543–54.
(13) Smeitink, J. A.; Zeviani, M.; Turnbull, D. M.; Jacobs, H. T. *Cell Metab* **2006**, *3* (1), 9–13.

NL901398T